

# RISAS: A Novel Rotation, Illumination, Scale Invariant Appearance and Shape Feature

Xiaoyang Li<sup>\*1</sup>, Kanzhi Wu<sup>\*2</sup>, Yong Liu<sup>1†</sup>, Ravindra Ranasinghe<sup>2</sup>, Gamini Dissanayake<sup>2</sup> and Rong Xiong<sup>1</sup>

**Abstract**—In this paper, we present a novel RGB-D feature, RISAS, which is robust to Rotation, Illumination and Scale variations through fusing Appearance and Shape information. We propose a keypoint detector which is able to extract information rich regions in both appearance and shape using a novel 3D information representation method in combination with grayscale information. We extend our recent work on Local Ordinal Intensity and Normal Descriptor(LOIND)[1], to further significantly improve its illumination, scale and rotation invariance using 1) a precise neighbourhood region selection method and 2) a more robust dominant orientation estimation. We also present a dataset for evaluation of RGB-D features, together with comprehensive experiments to illustrate the effectiveness of the proposed RGB-D feature when compared to SIFT[2], C-SHOT[3] and LOIND. We also show the use of RISAS for point cloud alignment associated with many robotics applications and demonstrate its effectiveness in a poorly illuminated environment when compared with SIFT and ORB[4].

## I. INTRODUCTION

In both fields of computer vision and robotics, feature matching is a fundamental problem in various applications such as object detection, image retrieval and robotic tasks such as vision based Simultaneous Localisation and Mapping (SLAM). Two essential steps critical to finding robust and reliable correspondences are 1) extracting discriminative keypoints and 2) building invariant descriptors. In the past decade, there has been enormous progress in developing robust features in 2-dimension image space such as SIFT(Scale Invariant Feature Descriptor)[2], SURF(Speed-Up Robust Descriptor)[5] and ORB(Oriented FAST and Rotated BRIEF)[6]. When rich texture information is available, these methods achieve excellent performance under significant variation to both scale and rotation. However, their performance can degrade drastically under illumination variations and environments with poor texture information.

With the development of low-cost, real-time depth sensors such as Kinect and Xtion, depth information of the environment can be easily obtained, thus it is now prudent to consider geometric information in building local descriptors. Spin Image[7] is one of the well-known 3D descriptors which

is widely used in 3D surface registration tasks. Rusu and et al. also made significant contributions to the literature in depth descriptors and proposed various methods such as PFH(Persistent Feature Histogram) and NARF(Normal Aligned Radial Feature). However, relying depth information alone makes the correspondence problem more challenging due to two reasons: 1) sensor information from Kinect and Xtion is general incomplete and 2) depth image is much less informative when compared with RGB/grayscale image, particularly in textured regions. Due to the complementarity nature of RGB/grayscale information and depth information, combining appearance and geometric information is a promising approach to building descriptors and improving matching performance. C-SHOT(Color Signature of Histogram and Orientation) and BRAND(Binary Robust Appearance and Normal Descriptor) are typical examples RGB-D descriptors. Compared with existing prominent 2D image features such as SIFT and SURF, a major limitation of current RGB-D detectors and descriptions is that they are designed without simultaneously considering effectiveness and both detection and description, which the present paper aims to address.

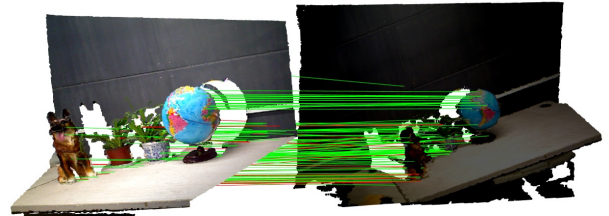


Fig. 1. Feature matching example using RISAS under severe rotation, scale, viewpoint and illumination variations. The correct matches are shown using green lines and incorrect matches are denoted by red lines.

In this paper, we present a novel Rotation, Illumination and Scale invariant Appearance and Shape feature (RISAS) which combines a discriminative RGB-D keypoint detector and an invariant feature descriptor. Fig.1 illustrates the ability of RISAS for obtaining correspondences under severe rotation, scale and illumination changes. Section. II reviews the related work in traditional RGB/grayscale local feature and descriptors, depth and RGB-D descriptors. In section III, We introduce the proposed keypoint detector computed using both grayscale image and a novel representation of depth image. Based on our previous work LOIND[1], a novel RGB-D descriptor with significant improvements is also explained in section III. In section IV, we present a

<sup>\*</sup>This indicates equal contribution of the first two authors.

<sup>1</sup>Xiaoyang Li, Yong Liu and Rong Xiong are with Institute of Cyber-Systems and Control, Zhejiang University, Hangzhou, 310027, China. lixiaoyang@163.com, yongliu, rxiong@iipc.zju.edu.cn

<sup>2</sup>Kanzhi Wu, Ravindra Ranasinghe and Gamini Dissanayake are with Centre for Autonomous Systems, University of Technology Sydney, Ultimo, 2007, Australia. kanzhi.wu, ravindra.ranasinghe, gamini.dissanayake@uts.edu.au

<sup>†</sup>Yong Liu is the corresponding author of this paper.

dataset specifically designed for RGB-D feature evaluation. RISAS is evaluated using four different criteria: illumination, scale, rotation and viewpoint and comparative experiments are conducted against SIFT, C-SHOT and the earlier version of LOIND. Comprehensive experiment results obtained using the proposed dataset as well as a public RGB-D dataset substantiate the superior performance of RISAS. We also adopted RISAS into point cloud alignment task. Under poor illuminated environments, compared with SIFT and ORB, our approach can achieve more consistent alignment results. Conclusion and future work are discussed in section V.

## II. RELATED WORK

There have been extensive research on feature detectors and descriptors for 2D images. The well-known SIFT feature, proposed by Lowe[2] with superior scale invariance, has been widely used in academic and industrial fields. Bay and et al.[5] presented SURF which follows a similar strategy to SIFT but requires less computation time and even outperforms SIFT with respect to repeatability and robustness. Because of the computational cost of using SIFT and SURF in real-time applications such as SLAM and tracking, binary descriptors such as BRIEF (Binary Robust Independent Elementary Features), BRISK (Binary Robust Invariant Scalable Keypoints) and ORB became popular since 2010. With less storage consumption and computation time, the most recent binary descriptor, ORB, is able to achieve comparable performance even compared with SIFT and SURF. Other types of descriptors are also proposed such as OSID (Ordinal-Spatial Intensity Distribution) [8] which computes the histogram to combine the relative ordering of the pixel intensities and spatial information.

Even though building descriptor from 2D images has been the focus in the past decade, it is not surprising that descriptors can also be constructed using 3D geometric information. In 1997, Johnson and Hebert [7] proposed Spin Image to match surfaces. Recently, with the development of low-cost RGB-D sensors, geometry information of the environment can be easily captured thus the importance of 3D shape descriptors have again been recognised. Various 3D descriptors have been proposed in the literature and currently available as implementations in the main public domain environment for dealing with point clouds, Point Cloud Library. Typical examples are PFH[9], NARF[10], VFH[11] and SHOT (Signatures of Histograms of Orientations)[12]. Guo and et al. presented a comprehensive performance evaluations and comparisons of the popular 3D local feature descriptors in [13]. Despite the progress in 3D shape descriptors, however, because of the fact that 3D shape(depth) information is not rich compared with RGB or grayscale image, a shape descriptor alone is able to provide reliable and robust feature matching results.

Lai and et al. [14], proved that by joining RGB and depth channels together, better recognition performance can be achieved for object recognitions? when compared with using one channel only. Tombari et al. introduced colour information into SHOT descriptor and proposed C-SHOT.

C-SHOT improves the feature matching accuracy and shows better performances for object recognition under cluttered environment. Nascimento and et al. proposed a binary RGB-D descriptor named BRAND (Binary Robust Appearance and Normals Descriptor)[15] which is invariant to rotation and scale transform. More recently, Feng and et al. proposed LOIND which encodes the texture and depth information into one descriptor using histogram representation which shows better performance compared with BRAND and C-SHOT on public datasets.

## III. METHOD

In this section, we describe the proposed Illumination, Scale and Rotation invariant Appearance and Shape feature, RISAS, in detailed. Compared with previous work[1], except for the further improvement on constructing a better descriptor, we proposed an RGB-D keypoint detector specifically designed for the new descriptor called LOIND+. The detector and LOIND+ are explained in detail in Section.III-A and Section.III-B.

### A. Keypoint Detector

In Feng’s work[1], the traditional keypoint detectors, Harris-Affine detector and Hessian-Affine detector[16], are applied in extracting regions of interest from gray-scale images even though both RGB and depth information are available. Because of the fact that depth information is not considered in detection phase, regions which are information-rich in depth channel are ignored due to the lack of texture information.

Considering depth information in keypoint detection helps in at least two aspects: 1) more number of keypoints are expected to be extracted and 2) more “discriminant” depth information will be used in building the descriptor and further improve the feature matching performance. In this paper, we propose an RGB-D keypoint detector method which is highly coupled with LOIND+ and the performances of LOIND+ is maximised when using the proposed detector.

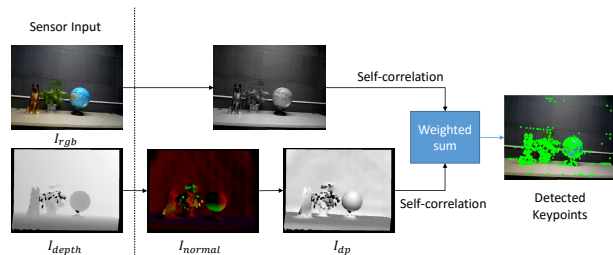


Fig. 2. Flowchart of the proposed RGB-D detector.  $I_{rgb}$  is the original RGB image and  $I_{grayscale}$  is the converted grayscale image.  $I_{normal}$  is the 3 channel normal vector image and  $I_{dp}$  is the computed dot product image.

The flowchart of the proposed detector is shown in Fig. 2 and the key steps are listed below:

- 1) For each point in the depth image  $I_{depth}$ , we calculate the surface normal vector. From the 3 components of the normal vector, we create the corresponding normal image  $I_{normal}$  with 3 channels.

- 2) Using  $I_{normal}$ , compute the three angles  $[\alpha, \beta, \gamma]$  between each normal vector and the  $[x, y, z]$  axis of the camera coordinate system respectively. Note that angles are in the continuous space in range  $[0, \pi]$ . The angle range  $[0, \pi]$  is segmented into 4 sector labelled with  $[1, 2, 3, 4]$  as shown in Fig.3 and each computed angle is mapped into one of these sectors. For example, normal vector  $\mathbf{n} = \left[ \frac{\sqrt{3}}{3}, \frac{\sqrt{3}}{3}, \frac{\sqrt{3}}{3} \right]$  has the  $[\alpha, \beta, \gamma] = [54.7^\circ, 54.7^\circ, 54.7^\circ]$  will be labelled as  $[2, 2, 2]$ ;
- 3) Using this labelled image, build a statistical histogram to capture the distribution of labels along each channel. From this histogram, we choose the highest entry and use the corresponding label  $[n_X, n_Y, n_Z]$  to represent the most frequent label where  $n_X, n_Y, n_Z \in [1, 2, 3, 4]$ . Using these 3 values, we define what we call the main normal vector  $\mathbf{n}_{main}$  of the depth image  $I_{depth}$ . This vector represents the relationship between the sensor and the scene;
- 4) Calculate the dot-product between the  $\mathbf{n}_{main}$  and each normal vector in  $I_{normal}$ . This dot product value is an indicator of how similar a given normal vector to the main normal vector which is approximately consistent when the sensor is pointing at the same scene from different angle. We then normalise the dot product value into range  $[0, 255]$ . Using this value, we create the novel dot-product image  $I_{dp}$  which can describe the variation of information in depth channel. This is highly coupled with the following descriptor construction step since the geometrical information is encoded using the dot-product value;
- 5) We adopt the similar principle as in Harris detector to compute the response value  $E(u, v)$ . We use both the grayscale image  $I_{grayscale}$  and the dot product image  $I_{dp}$  to compute the response value and set a threshold to select the point which shows an extreme value in the weighted sum of response values, as shown in Eq.1:

$$E(u, v) = \sum_{x, y} \omega(x, y) [\alpha (I(x + u, y + v) - I(x, y))^2 + (1 - \alpha) (P(x + u, y + v) - P(x, y))^2] \quad (1)$$

where  $\omega(x, y)$  is the window function centred at  $(x, y)$  which is a Gaussian function in this paper.  $I(u, v)$  is the intensity value at  $(u, v)$  and  $P(u, v)$  is the normalised dot product value at  $(u, v)$ . Since the RGB information is more accuracy compared with noisy depth information, in this paper,  $\alpha$  is set to be 0.8.

Using the proposed approach, the regions which are lack of depth information are first eliminated. Also by introducing the novel representation of depth image,  $I_{dp}$ , we can extract keypoints from not only appearance information rich region but also geometry information rich region. The designed detector is highly coupled with the principle of LOIND+ and drastically improves the performance of LOIND+ under different scenarios and the detailed results will be shown in

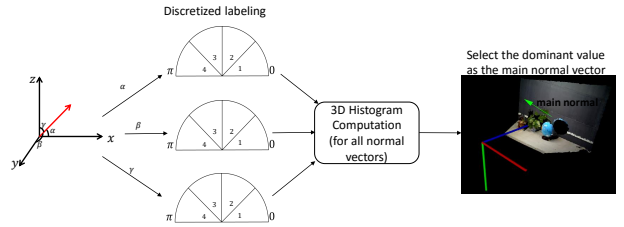


Fig. 3. Flowchart of calculating the main normal.

## Section.IV.

### B. LOIND+

#### 1) Scale Estimation and Neighbourhood Region Selection:

In grayscale image, the scale of the keypoint is estimated by finding the extreme value in scale space using image pyramid, such as SIFT[2] and SURF[5]. However, the scale invariance will be degraded once the texture information in the neighbourhood is poor or under large illumination variations. With the development of modern RGB-D sensors such as Kinect and Xtion, the scale can be easily measured using the depth information captured from the sensor. In both LOIND[1] and BRAND[15], the following empirical equation is applied by assuming the linear relationship between depth measurement  $d$  and scale  $s$  in range  $[2, 8]$  meters.

$$s = \max(0.2, \frac{3.8 - 0.4 \max(2, d)}{3}) \quad (2)$$

One obvious problem in Eq. 2 is that it is not applicable to closer range within 2 meters where the sensor is frequently used. After  $s$  is estimated, the neighbourhood region that is used to build the descriptor is selected with radius  $R$  which varies w.r.t.  $s$  in a linear relationship, as shown in [1][15]. However, there are two facts ignored in selecting the neighbourhood region: 1) the depth resolution is not constant and decreases with increasing distance to the sensor [17], thus the linear assumption no longer holds; 2) select neighbourhood region using radius  $R$  without considering the geometric information in the neighbourhood is likely to include irrelevant background points, shown in Fig.4. In order to address this, we present a more accurate neighbourhood region selection method for building descriptor:



Fig. 4. Neighbourhood selection: The default strategy (left) selects the whole region (shown in red) which covers both foreground and background area. However, the introduced background points are not necessary for building the local descriptor. Our approach (right) eliminates the background points (shown in blue) and constructs the descriptor using the foreground (shown in red) only which achieves more robust descriptor matching performances.

- 1) Based on Eq.2, initial value of the scale  $s$  is estimated and the radius  $R$  of the patch is computed using Eq.3.

$$R = \left( -5 + 25 * \min \left( 3, \frac{\max(0.2.s_{max})}{\max(0.2.s_{min})} \right) \right) * s \quad (3)$$

Where  $s_{max}$  and  $s_{min}$  are the maximum and minimum scale values in the image. Here we denote the patch centred at keypoint  $k_i$  in 2D image space as  $\mathbf{P}^{uv}(k_i)$  and the corresponding patch in 3D point cloud space is represented as  $\mathbf{P}^{xyz}(k_i)$ ;

- 2) For each point  $p \in \mathbf{P}^{xyz}(k_i)$ , we remove the outlier neighbouring points which are relatively far away from the keypoint  $k_i$  according to Eq.4. This simple elimination step enables significant improvements with LOIND+ descriptor.

$$f(p) = \begin{cases} 1 & \text{if } \|p - k_i\| < t \\ 0 & \text{otherwise} \end{cases} \quad (4)$$

where  $t$  is the threshold and set to be 0.1 meter in this work. We only keep the neighbouring points with  $f(p) = 1$ ;

- 3) We conduct ellipsoid fitting for the processed 3D neighbouring points  $\bar{\mathbf{P}}^{xyz}(k_i)$  based on the following equation.

$$\frac{(x - k_{ix})^2}{a^2} + \frac{(y - k_{iy})^2}{b^2} + \frac{(z - k_{iz})^2}{c^2} = 1 \quad (5)$$

where  $a, b$  and  $c$  are the length of the axes. We project the 3D ellipsoid into the image space for the new accurate patch  $\mathbf{P}$  with radius  $\bar{R}$  for further descriptor construction.

2) *Orientation Estimation:* In order to achieve robust rotation invariance, the traditional methods use the texture information which can fail under severe illumination variations. In our previous work, LOIND[1], the dominant orientation  $\theta$  is computed from the depth information rather than the appearance information and works reasonably well under different variations. However, the proposed approach is not computation efficient and more importantly,  $\theta$  is sensitive to the noise in neighbourhood region where the normal vectors are similar to each other.

In this work, still using depth information, we propose an alternative novel dominant orientation estimation algorithm which is more robust and efficient compared with LOIND[1], as shown in detail below:

- 1) Given the processed 2D patch  $\bar{\mathbf{P}}^{uv}$  and 3D patch  $\bar{\mathbf{P}}^{xyz}$ , we adopt PCA to compute the eigenvalues  $[e_1, e_2, e_3]$  (in *descending* order) and corresponding eigenvectors  $[\mathbf{v}_1, \mathbf{v}_2, \mathbf{v}_3]$ .
- 2) Given the eigenvectors  $[\mathbf{v}_1, \mathbf{v}_2, \mathbf{v}_3]$ , here we provide a approximation method for computing the 3D dominant

orientation  $d_{3D}$  of the patch in below:

$$d_{3D} = \begin{cases} \frac{\mathbf{v}_1 + \mathbf{v}_2}{|\mathbf{v}_1 + \mathbf{v}_2|} & \text{if } (e_2 > \tau e_1) \wedge (e_3 \leq \tau e_1) \\ \frac{\mathbf{v}_1 + \mathbf{v}_2 + \mathbf{v}_3}{|\mathbf{v}_1 + \mathbf{v}_2 + \mathbf{v}_3|} & \text{if } (e_2 > \tau e_1) \wedge (e_3 > \tau e_1) \\ \mathbf{v}_1 & \text{others} \end{cases} \quad (6)$$

where  $\tau$  is set within  $[0, 1]$ . If the  $e_1$  is significantly larger than other two, the 3D dominant orientation is set to be the corresponding eigenvector  $\mathbf{v}_1$ . If  $e_2$  is closer to  $e_1$ , both eigenvector  $\mathbf{v}_1$  and  $\mathbf{v}_2$  are considered in computing the dominant orientation. If further both  $e_1$  and  $e_2$  are closer to  $e_1$  which means no clear differences between 3 eigenvalues, all 3 eigenvector are used in computing  $d_{3D}$ . Threshold  $\tau$  determines when the other two eigenvalues  $e_2$  and  $e_3$  can be regarded as ‘‘closer’’ enough to the largest eigenvalue  $e_1$  which is set to be 0.8 in this paper.

- 3) Project the 3D dominant direction  $d_{3D}$  into the image plane and get the 2D dominant direction  $d_{2D}$ . The angle  $\theta$  between  $d_{2D}$  and  $u$  axis in image space is set to be the dominant orientation.

3) *Descriptor Construction:* Based on the results from the above steps, we can construct the descriptor of keypoint  $k_i = [u, v]$  using the neighbourhood region with radius  $R$  and the orientation  $\theta$ . We still follow on the main idea of LOIND[1]. The descriptor is based on the relative order information in both grayscale and depth channels. The descriptor is constructed in a three-dimensional space, as show in Fig. 5 below where  $[x, y, z]$  axes denote the spatial labelling, the intensity labelling and the angles labelling respectively.

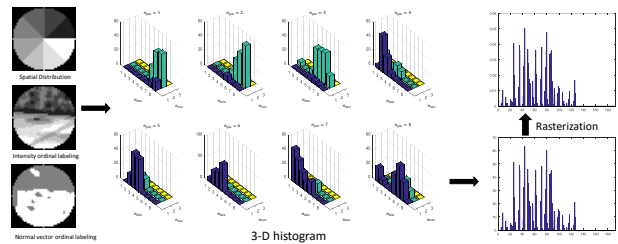


Fig. 5. Flowchart of the RGB-D descriptor.

#### - Spatial Distribution Encoding

For spatial distribution, the pixels in the region  $(u, v, R, \theta)$  are labeled based on  $n_{pie}$  equal-size spatial sectors. With larger number of pies, the descriptor is supposed to be more discriminative and also more time-consuming for both construction and matching. In previous work, LOIND[1],  $n_{pie}$  is set to be 8 which shows a good trade-off between its pros and cons and we use the same value in this work.

#### - Grayscale Information Encoding

Instead of constructing the descriptor in the absolute intensity space, we build the statistical histogram using the relative intensity with respect to the intensity value

of the keypoint. According to the rank of all the pixels in the patch, we group the intensity values into  $n_{bin}$  equally sized bins. For example, given 100 intensity levels and 10 bins, each bin has 10 intensity levels (i.e., orderings of  $[1, 10], [11, 20], \dots, [91, 100]$  ).

#### - Geometrical Information Encoding

Given the normal vector of each point, we first compute the dot product between the normal vector of the selected keypoint  $\mathbf{n}_{p_k}$  and the normal vector each point in the neighbourhood patch  $\mathbf{n}_{p_i}$ .

$$\rho_i = |\langle \mathbf{n}_{p_k}, \mathbf{n}_{p_i} \rangle| \quad (7)$$

Due to the fact that normal vectors from small patches are similar to each other, thus the distribution of  $\rho_i$  is highly unbalanced where the majority of  $\rho_i$  will fall into the range close to 1. In this work, we set a threshold  $\bar{\rho} = 0.9$  and any  $\rho_i \geq \bar{\rho}$  will be grouped into a special case. Other remaining dot product results will be ranked and grouped into  $n_{vec}$  bins and the points will be labelled based on the group they belong to respectively. Therefore, in normal vector space encoding, there are overall  $n_{vec} + 1$  labels and in our work  $n_{vec}$  is set to be 2.

In the end, we can encode every neighbouring pixel in the patch as  $(i, j, k)$ , and then build a three-dimensional statistical histogram to get a 192-dimensional normalised descriptor for the patch.

## IV. EXPERIMENTS AND RESULTS

In this section, in order to evaluate the proposed RGB-D feature on different criterion independently, we constructed an RGB-D descriptor evaluation dataset<sup>1</sup>. We present the comparative results of RISAS against SIFT, CSHOT and LOIND on the constructed dataset. We also compared these methods on the public RGB-D dataset which is originally designed for object detection<sup>2</sup>. Furthermore, we demonstrate the result for point cloud alignment using RISAS as an application. Under poor illuminated environment, our algorithm achieves more consistent results compared with using SIFT and ORB.

### A. Performance Evaluation

1) *Evaluation Metric*: We adopt the same evaluation metric proposed by Mikolajczyk and Schmid[18]. We first extract interesting points from the two frames and compute the descriptors for all keypoints. Nearest neighbour distance ratio (NNDR) is used to establish the correspondences between keypoints between different images. In the end, we can use the formula below to determinate whether the correspondence is correct:

$$\|p_i - (\mathbf{R}p_j + \mathbf{t})\| \leq \tau \quad (8)$$

<sup>1</sup>The dataset can be downloaded from <http://kanzhi.me/rgbd-descriptor-dataset/>

<sup>2</sup><http://rgbd-dataset.cs.washington.edu/>

where  $p_i$  and  $p_j$  are 3d points from two frame  $i$  and  $j$ .  $\mathbf{R}$  and  $\mathbf{t}$  denote relative rotation and translation between frame  $i$  and  $j$ . If the projected error is less than  $\tau$ , the match is regarded as a correct one and  $\tau$  is set to be 0.05 m in our work.

2) *Dataset and Results in Detail*: In this section, we demonstrate the comparison results against SIFT, CSHOT and LOIND on the public dataset and our dataset to validate the effectiveness of RISAS<sup>3</sup>.

#### - Scale Invariance

In this experiment, we collect 10 frames of images with the variations in  $z$  axis of the sensor coordinate system. The first frame which captured at 1.1 m is selected as the reference image and all other images are captured backwards every 0.1 m. We select 500 matches with highest matching scores as the total matches. We decide whether the match is correct or not according to Eq.8. The matching accuracy is shown in Fig.6. The proposed RISAS shows significant higher percentage of inliers compared with SIFT and LOIND and slightly improvement compared with CSHOT.

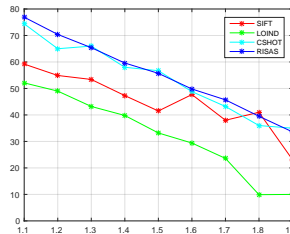


Fig. 6. Matching performance of SIFT, LOIND, CSHOT and RISAS under scale variations.

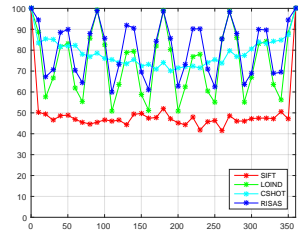


Fig. 7. Matching performance of SIFT, LOIND, CSHOT and RISAS under synthetic rotation variations.

#### - Rotation Invariance

We evaluate the performance of RISAS under 2 types of rotation transformations: synthetic in-plane rotation and actual 3D rotation. We generated synthetic data by rotating the original image every  $10^\circ$  and added additional Gaussian noise to the rotated image. Fig.7 shows that RISAS achieves comparable performance compared with CSHOT and outperforms SIFT and LOIND significantly.

We also evaluate RISAS under actual 3D rotation shown in Fig. 8 and compared against SIFT, LOIND and CSHOT and the precision-recall curves are presented in Fig.9. RISAS shows similar performance compared with CSHOT while achieve significant improvements compared with SIFT and LOIND.

#### - Illumination Invariance

In order to validate the performance of RISAS under illumination variations, we constructed a dataset which consists 4 different levels of synthetic illumination variations: 1) square 2) square root 3) cube and 4) cube root, shown in the left column in Fig.10. We

<sup>3</sup>SIFT has its own keypoint detector. For CSHOT and LOIND, we apply the proposed detector in this work to both of them.



Fig. 8. Example images of 3D rotations.

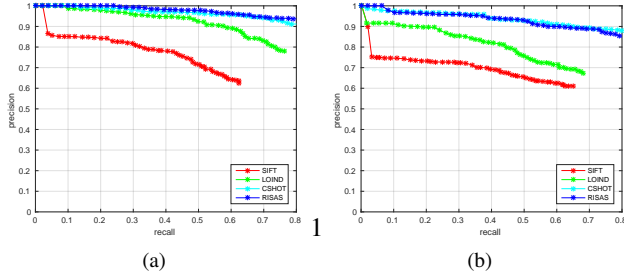


Fig. 9. Precision-Recall curves corresponding to images shown in Fig. 8.

also utilise neutral density filter to simulate the natural illumination variation. The Precision-Recall curves corresponding to the left column images are also shown in Fig.10 where the proposed RISAS shows significant better performance compared with SIFT, LOIND and especially CSHOT.

#### - Viewpoint Invariance

In this section, we collected overall 24 images by moving the sensor around the objects in  $60^\circ$  at 0.7 meters away from the objects. In order to compute the ground-truth transformation across each pair of frames and further evaluate the performance of descriptors, we adopt RGBD-SLAM[19] to compute the optimised poses and regard the optimised poses as the ground-truth. The Precision-Recall curves of 4 pairs of images are shown in Fig. 11. Again, the proposed RISAS shows significantly better performance compared with C-SHOT, SIFT and LOIND.

3) *Public Dataset Evaluation:* Except for the proposed dataset, we also validate RISAS on public RGB-D scene dataset. We select the table\_1 dataset from RGB-D scene dataset. Parts of the images and results are presented in Fig.12. RISAS also achieves better results compared with SIFT, C-SHOT and LOIND.

#### B. Application: Point Cloud Alignment

In order to validate the performance of the proposed RGB-D feature, we apply RISAS into the point cloud alignment task. During the data collection, we turned off the indoor light thus creates significant illumination changes in the environment. We match features across each observations using SIFT, ORB and RISAS and compute the relative poses. The point clouds from each steps are aligned and Iterative Closest Point is used to obtain the final alignment results. The aligned clouds are visualised in Fig.13. Using SIFT feature shows obvious error in the top right corner of the map. Result

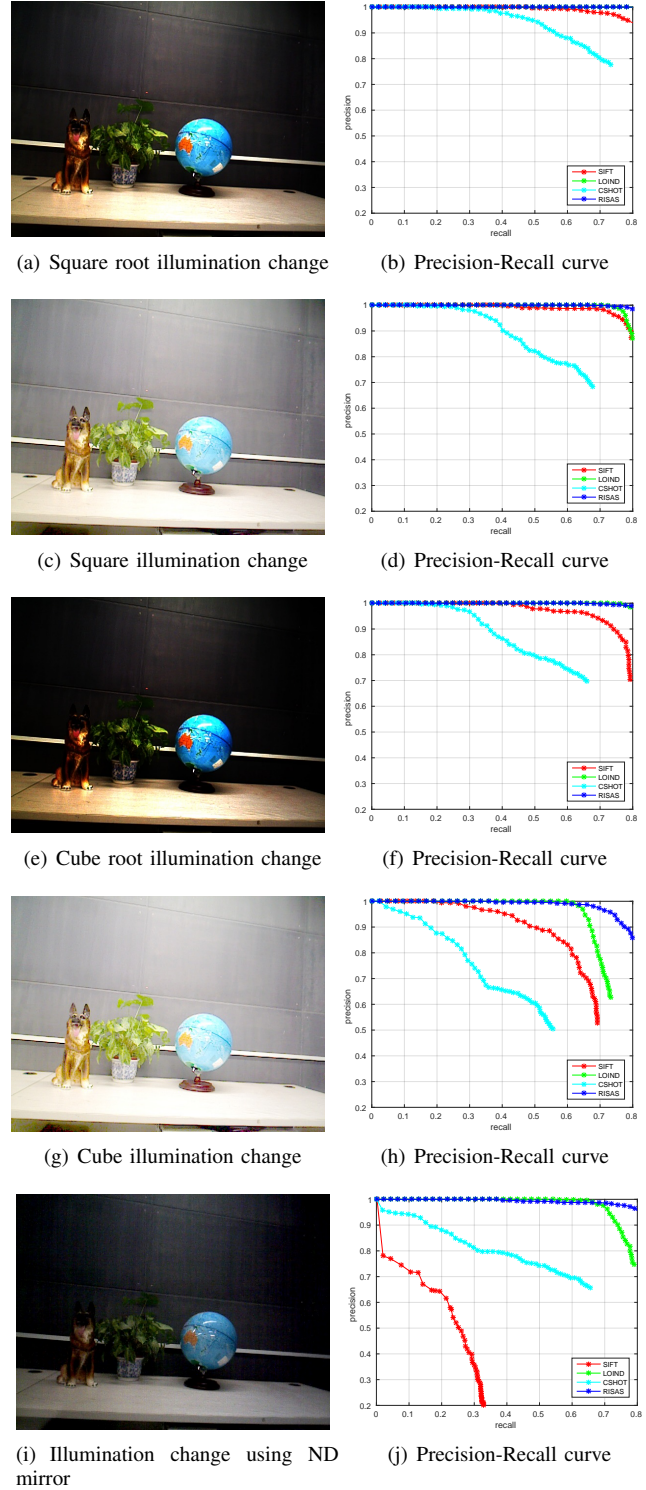


Fig. 10. RISAS evaluation under illumination variations.

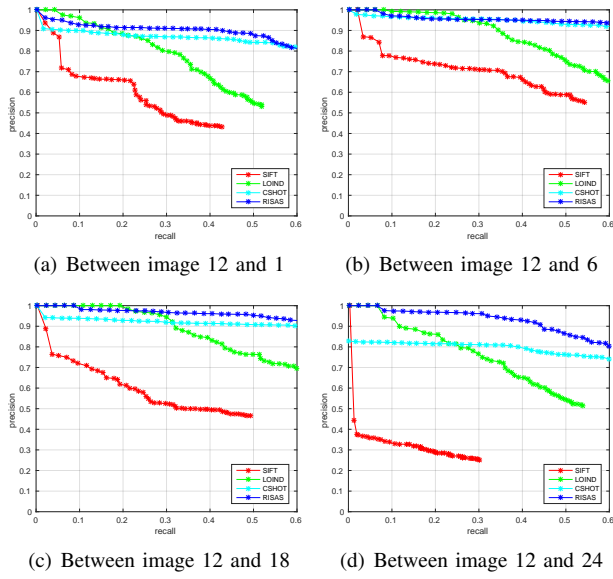


Fig. 11. Precision-Recall curves under viewpoint variations.

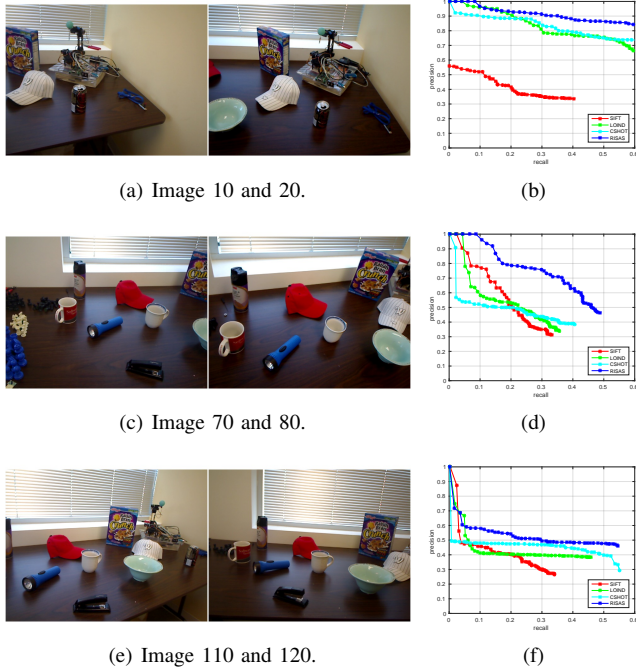


Fig. 12. Evaluation results on RGB-D scene dataset table\_1. The left column shows the input images and the right column shows in the corresponding Precision-Recall curve.

from ORB feature shows slightly offset in both corners. RISAS provides the best aligned point cloud as shown in Fig.13(c).

## V. CONCLUSION

This paper presents, as far as we know, the first RGB-D feature which consists a highly coupled a RGB-D key-point detector and descriptor. RISAS is invariant to multiple variations include illumination, scale, rotation and viewpoint. A novel 3D representation, dot-product image, is proposed

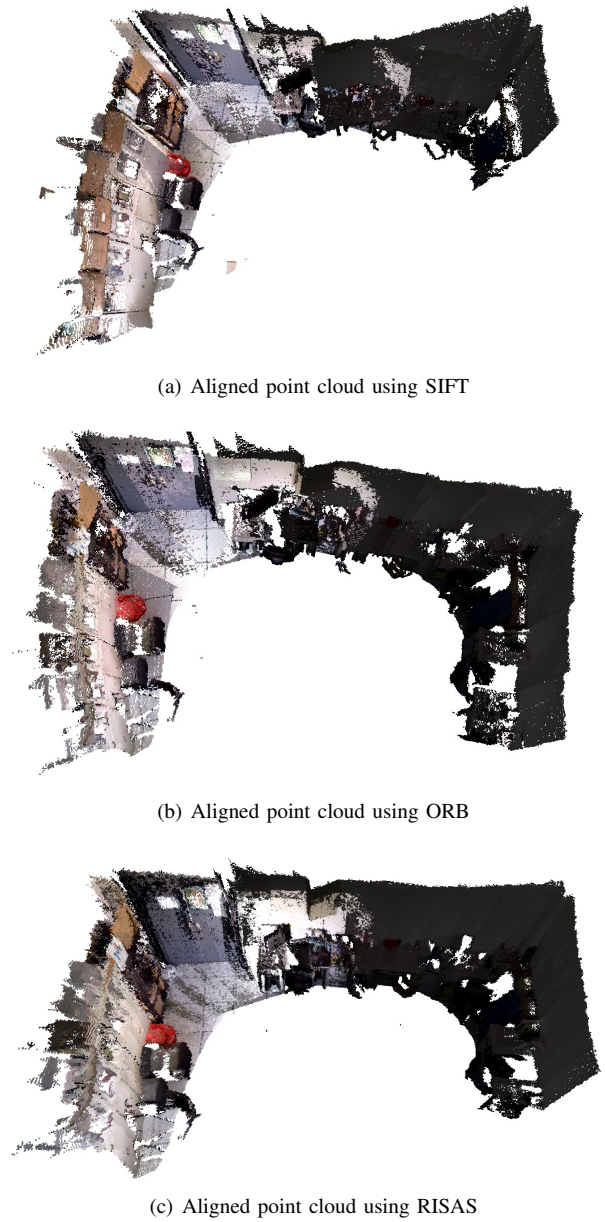


Fig. 13. Point cloud alignment under illumination variations.

based on original depth image and it is further combined with grayscale image to extract the interest keypoints using the similar principle as Harris detector. We also propose a novel RGB-D descriptor, LOIND+, which significantly improves the previous LOIND descriptor on every aspect. We construct an RGB-D dataset specifically designed for RGB-D feature evaluation. Through comprehensive comparisons, RISAS shows exceptional performance not only on the proposed dataset but also on publicly available datasets such as RGB-D scene dataset. Through adopting RISAS into point cloud alignment task, our approach shows more consistent result compared with using SIFT and ORB.

## ACKNOWLEDGEMENT

This work is supported by the Joint Research Centre for Robotics Research between Zhejiang University (ZJU) and University of Technology Sydney (UTS). Kanzhi Wu is also supported by University of Technology Sydney – China Scholarship Council (UTS–CSC) International Research Scholarship.

## REFERENCES

- [1] G. Feng, Y. Liu, and Y. Liao, “Loind: An illumination and scale invariant rgb-d descriptor,” in *Proc. IEEE International Conference on Robotics and Automation (ICRA’ 2015)*, May 2015, pp. 1893–1898.
- [2] D. Lowe, “Distinctive image features from scale-invariant keypoints,” *International Journal of Computer Vision*, vol. 60, no. 2, pp. 91–110, 2004.
- [3] F. Tombari, S. Salti, and L. Di Stefano, “A combined texture-shape descriptor for enhanced 3d feature matching,” in *Proc. IEEE International Conference on Image Processing (ICIP’2011)*, Sep 2011, pp. 809–812.
- [4] E. Rublee, V. Rabaud, K. Konolige, and G. Bradski, “Orb: an efficient alternative to sift or surf,” in *IEEE International Conference on Computer Vision (ICCV’2011)*. IEEE, 2011, pp. 2564–2571.
- [5] H. Bay, T. Tuytelaars, and L. Van Gool, “Surf: Speeded up robust features,” in *Proc. European Conference on Computer Vision (ECCV’ 2006)*, 2006, vol. 3951, pp. 404–417.
- [6] E. Rublee, V. Rabaud, K. Konolige, and G. Bradski, “Orb: An efficient alternative to sift or surf,” in *Proc. IEEE International Conference on Computer Vision (ICCV’ 2011)*, Nov 2011, pp. 2564–2571.
- [7] A. Johnson and M. Hebert, “Using spin images for efficient object recognition in cluttered 3d scenes,” *IEEE Transaction on Pattern Analysis and Machine Intelligence (PAMI)*, vol. 21, no. 5, pp. 433–449, May 1999.
- [8] F. Tang, S. H. Lim, N. L. Chang, and H. Tao, “A novel feature descriptor invariant to complex brightness changes,” in *IEEE International Conference on Computer Vision and Pattern Recognition (CVPR’2009)*. IEEE, 2009, pp. 2631–2638.
- [9] R. B. Rusu, Z. C. Marton, N. Blodow, and M. Beetz, “Persistent point feature histograms for 3d point clouds,” in *Proc. International Conference on Intelligent Autonomous Systems (IAS’2008)*, 2008.
- [10] K. K. Bastian Steder, Radu Bogdan Rusu and W. Burgard, “Narf: 3d range image features for object recognition,” in *Proc. Workshop on Defining and Solving Realistic Perception Problems at IEEE/RSJ International Conference on Intelligent Robots and Systems (IROS’2010)*, 2010.
- [11] R. Rusu, G. Bradski, R. Thibaux, and J. Hsu, “Fast 3d recognition and pose using the viewpoint feature histogram,” in *Proc. IEEE/RSJ International Conference on Intelligent Robots and Systems (IROS’2010)*, Oct 2010, pp. 2155–2162.
- [12] F. Tombari, S. Salti, and L. Di Stefano, “Unique signatures of histograms for local surface description,” in *Proc. European Conference on Computer Vision (ECCV’2010)*, 2010, pp. 356–369.
- [13] Y. Guo, M. Bennamoun, F. Sohel, M. Lu, J. Wan, and N. Kwok, “A comprehensive performance evaluation of 3d local feature descriptors,” *International Journal of Computer Vision*, pp. 1–24, 2015.
- [14] K. Lai, L. Bo, X. Ren, and D. Fox, “Sparse distance learning for object recognition combining rgb and depth information,” in *Proc. IEEE International Conference on Robotics and Automation (ICRA’2011)*, May 2011, pp. 4007–4013.
- [15] E. Nascimento, G. Oliveira, M. Campos, A. Vieira, and W. Schwartz, “Brand: A robust appearance and depth descriptor for rgb-d images,” in *Proc. IEEE/RSJ International Conference on Intelligent Robots and Systems (IROS’ 2012)*, Oct 2012, pp. 1720–1726.
- [16] K. Mikolajczyk, T. Tuytelaars, C. Schmid, A. Zisserman, J. Matas, F. Schaffalitzky, T. Kadir, and L. V. Gool, “A comparison of affine region detectors,” *International Journal of Computer Vision*, vol. 65, no. 1, pp. 43–72, 2005.
- [17] K. Khoshelham, “Accuracy analysis of kinect depth data,” in *International Archives of the Photogrammetry, Remote Sensing and Spatial Information Sciences*, vol. 38, 2011, p. 1.
- [18] K. Mikolajczyk and C. Schmid, “A performance evaluation of local descriptors,” *IEEE Transactions on Pattern Analysis and Machine Intelligence*, vol. 27, no. 10, pp. 1615–1630, 2005.
- [19] F. Endres, J. Hess, J. Sturm, D. Cremers, and W. Burgard, “3-d mapping with an rgb-d camera,” *Robotics, IEEE Transactions on*, vol. 30, no. 1, pp. 177–187, Feb 2014.